ELSEVIER

Catalysis Today 29 (1996) 221–228

CATALYSIS TODAY

Preparation of nickel–tungstate catalysts by a novel impregnation method

Y. Yoshimura [a,*], T. Sato [a], H. Shimada [a], N. Matsubayashi [a], M Imamura [a], A. Nishijima [a], M. Higo [b], S. Yoshitomi [b]

[a] *National Institute of Materials and Chemical Research, Tsukuba 305, Japan*
[b] *Shibaura Institute of Technology, Shibaura, Tokyo 108, Japan*

Abstract

Nickel–tungstate/γ-alumina (NiW) catalysts were prepared by an incipient wetness impregnation method using citric acid as a complexing agent. Citric acid has been used by our research group in preparing cobalt–molybdate and nickel–molybdate catalysts. The extended X-ray absorption fine structure (EXAFS) data of the impregnating solutions indicated that citric acid contributes to the formation of polytungstate anions that are smaller than the dodecatungstate ions formed when conventional ammoniacal solutions are used. Sulfided NiW catalysts prepared by using citric acid showed higher hydrogenation activity and hydrogenation selectivity than NiW catalysts prepared using the conventional ammoniacal solutions.

Keywords: Nickel–tungstate catalysts; Citric acide; EXAFS; TPR; Thermodynamics

1. Introduction

Tightened environmental regulations on emissions include low aromatic and sulfur specifications for diesel fuels. Catalysts for aromatic saturation are classified into two groups: conventional sulfide catalysts, such as NiMo and NiW, and sulfur-tolerant noble-metal catalysts. The former catalysts are preferred for moderate-level aromatic saturation, but the latter catalysts for deep aromatic saturation. Thus, a combination of these catalysts is a promising option in controlling the aromatic contents of hydrotreated diesel fuels. Though high-severity hydrotreating is necessary for conventional sulfide catalysts, in integrated hydrotreatment systems in which these catalysts are used in the first stage and sulfur-tolerant noble-metal catalysts are used in the second stage, the hydrogenation performance of these sulfide catalysts affects the performances and life of these noble-metal catalysts. Tungstate catalysts are known to be highly active in the hydrotreating/hydrocracking of middle distillates and in the upgrading of coal-derived oils, which contain low concentrations of sulfur [1,2]. In spite of their price and limited reaction atmospheres [3,4] when compared with NiMo catalysts, NiW catalysts are advantageous because their potential activity in aromatic saturation is quite high. Therefore, accelerating the development of NiW catalysts would impact their use

* Corresponding author.

0920-5861/96/$32.00
SSDI 0920-5861(95)00275-8

as aromatic saturation catalysts. This was the motive for this study.

In this study we prepared NiW impregnating solutions by using citric acid as the complexing agent [5,6], one that we have previously used in preparing cobalt–molybdate and nickel–molybdate catalysts. We then determined the tungsten structure of the impregnating solutions and the resulting sulfided nickel–tungstate/γ-alumina (NiW) catalysts by using extended X-ray absorption fine structure (EXAFS) analysis and X-ray photoelectron spectroscopy (XPS). We also characterized the sulfided NiW catalysts by using a temperature-programmed reduction (TPR) method. We also looked at the effects of citric acid addition on the hydrogenation activity (HYG) and hydrogenation selectivity of the catalysts. Finally, to better understand the structural changes in the active components during sulfidation and reduction, we carried out a thermodynamic analysis.

2. Experimental

The NiW catalysts were prepared by an incipient wetness impregnation method. We prepared two types of NiW catalysts using two different impregnating aqueous solutions: ammoniacal (am), which is commonly used to prepare NiW catalysts, and citrate (cit), which is used to control the active phase structure of NiW catalysts. We designated these two catalysts as NiW(am) and NiW(cit), respectively. The am solutions were prepared using a solution of ammonium tungstate $(NH_4)_6H_2W_{12}O_{40} \cdot nH_2O$ (the solution was 50.7 wt.% WO_3) and nickel nitrate. The cit solutions were prepared using the tungstate solution, nickel carbonate, and citric acid (at a citric acid:Ni molar ratio of 1.0). The γ-Al_2O_3 was supplied by Catalysts & Chemicals Industries Co., Ltd. and had a surface area of 209 m^2/g and a pore volume of 0.81 cm^3/g. The impregnated catalysts were dried at 393 K for 4 h (hereafter we designated the catalysts at this stage by a D) and then calcined at 773 K (which is the standard temperature for catalysts used in TPR and EXAFS analyses, and in hydrogenation selectivity tests) for 3 h (designated by CL) in dry air (at a flow-rate of 3 l/min). We then took some of the dried NiW(cit) catalyst and pyrolyzed it at several temperatures (e.g., 673, 773, and 873 K) for 3 h in dry nitrogen (designated as PY). Prior to sulfidation, some of the calcined catalyst was reduced at 773 K for 2 h (designated as CL-R). The amounts of active components for the NiW catalyst were 4.2 wt.% NiO and 29.0 wt.% WO_3, and for the W catalysts 29.0 wt.% WO_3. These NiW catalysts were then sulfided with a gas containing hydrogen and hydrogen sulfide (H_2S–H_2; 5:95, v/v) at 673 K for 2 h prior to characterization and test reactions for evaluating the hydrogenation and hydrocracking activities.

The EXAFS measurements of the impregnating solutions and sulfided catalysts (at the beam lines of BL 10B and 7C) were done at the Photon Factory of the National Laboratory for High Energy Physics. The XPS measurements were performed on pulverized samples of the catalysts using an XPS (PHI-5400MC).

In the TPR measurements, a portion of the sulfided catalysts (0.3 g, and a particle diameter of 74–149 μm) was packed in a quartz reactor, and reduced using a reducing gas that contained hydrogen and nitrogen (H_2–N_2; 1:1, v/v) at a heating rate of 5 K/min, a temperature up to 1073 K, and a flow-rate of 0.4 l (NTP)/min. The composition of the product gases was monitored using a mass spectrometer. To better understand the reduction and sulfidation behavior of the active components during the TPR and sulfidation experiments, respectively, we determined the chemical potential diagrams [7], using a thermodynamic data base [8,9].

To evaluate the initial hydrogenation (HYG) activities of the NiW catalysts, we hydrogenated a 1-methylnaphthalene diluting solution with *n*-hexadecane (30% 1-MN and 70% *n*-hexadecane) in a tube-bomb batch reactor (volume capacity of 50 cm^3) for 1 h at 573 K under an initial H_2 pressure of 3.0 MPa. To evaluate the

HYG/hydrocracking (HYC) selectivity, we hydrogenated diphenylmethane (DPM) in a tube-bomb batch reactor for 1 h at 673 K under an initial H_2 pressure of 6.9 MPa. The yield of dicyclohexylmethane and benzylcyclohexane showed the level of HYG activity, and the yield of benzene and toluene showed that of HYC. Taking into account the released H_2S from the sulfided catalysts, no extra sulfur compounds or H_2S were added to the batch reactor.

3. Results and discussion

3.1. Structure of tungsten in the impregnating solutions

Fig. 1 shows the Fourier transforms of the EXAFS spectra (W L_{III}-edge) for the impregnating NiW(am) and NiW(cit) solutions as well as the starting W(am) solution. Three main peaks occurred at 0.17, 0.20, and 0.39 nm for the NiW(am) solution, which correspond to the terminal W–O, bridging W–O, and W–W coordination of dodecatungstate ions, $[H_2(W_{12}O_{40})]^{6-}$ [10], respectively. There are only slight differences in the EXAFS spectra between the starting W(am) solution (pH 3.3) and the NiW(am) solution (pH 1.9). This indicates that the structure of most of the dodecatungstate ions was maintained in the pH range 1.9–3.3; in other words, there was little possibility of depolymerization of the dodecatungstate ions in this pH range. On the contrary, there were significant differences between the spectra for the starting W(am) solution and the NiW(cit) solution (pH 3.3), namely, the intensities of the peaks at 0.20 and 0.39 nm decreased, and that at 0.17 nm increased. The reason for these changes is that the coordination of citrate ligands to the distorted WO_6 octahedra in dodecatungstate ions might have resulted in the depolymerization of some of the ions and in the formation of relatively small polyanions (i.e., smaller than the dodecatungstate ions formed when ammoniacal solutions are used). This coordination was promoted by the Ni^{2+}–citrate interactions.

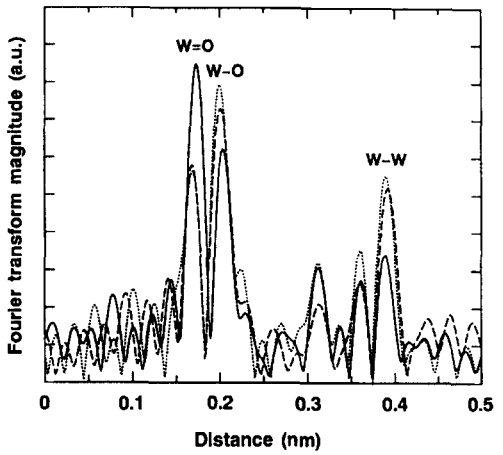

Fig. 1. Fourier transforms of tungsten EXAFS spectra for the NiW impregnation solutions (k^3-weighted, $\Delta k = 14.4$ ($3.75 < k < 17.75$ Å^{-1}): ammoniacal W(am) solution (· · ·), ammoniacal NiW(am) solution (– – –), and NiW(cit) (—) solution using citric acid.

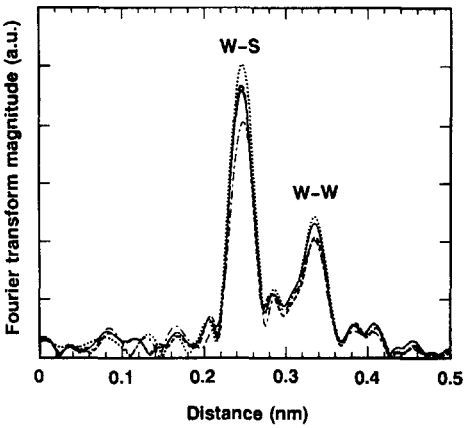

Fig. 2. Fourier transforms of tungsten EXAFS spectra for the sulfided NiW(cit) and NiW(am) catalysts (k^3-weighted, $\Delta k = 14.4$ ($3.5 < k < 17.5$ Å^{-1}): NiW(cit) (D) (· · ·), NiW(cit) (D-CL) (—), NiW(cit) (D-PY) (— — —), and NiW(am) (D-CL) (– – –) catalysts.

3.2. Structure of tungsten in the sulfided NiW catalysts

Fig. 2 shows the Fourier transforms of the EXAFS spectra (W L_{III}-edge) for the sulfided NiW(am) (D-CL), NiW(cit) (D-CL), NiW(cit) (D), and NiW(cit) (D-PY) catalysts. For each of the catalysts, two main peaks occurred at 0.241 and 0.315 nm, which correspond to the first W–S and W–W coordinations in WS_2 crystal-

lites [11], respectively. The highest intensities of the W–S and W–W peaks were for the sulfided NiW (D) catalyst, indicating that this catalyst had the most extensive lateral growth of WS_2-like crystallites (i.e., growth of the (002) planes) even though carbonaceous material (1.2 wt.% carbon) was remained on the catalyst. Not only did such carbonaceous material not interfere with the diffusion of H_2S, it also might have minimized the interactions between the active components and the γ-Al_2O_3 support. Despite the similar intensities for the W–W and W–S peaks for both the sulfided NiW(cit) (D-CL) and NiW(am) (D-CL) catalysts, the W–W peak intensity was higher for the NiW(cit) than for the NiW(am). This indicates that the WS_2-like crystallites grew more in the lateral direction in the NiW(cit) (D-CL) catalyst than in the NiW(am) (D-CL) catalyst, possibly due to the smaller tungstate polyanions in the NiW(cit) impregnating solution. The lowest intensities of the W–S and W–W peaks were found for the sulfided NiW(cit) (D-PY) catalyst, on which 1.2 wt.% carbon remained. This indicates that the refractory carbonaceous material covered the oxidic precursors and retarded sulfidation, causing WS_2-like crystallites to form.

3.3. Surface composition of the sulfided NiW catalysts

Table 1 shows the surface composition of the sulfided NiW catalysts determined by using XPS. By comparing the sulfided NiW(am) (D-CL) and NiW(cit) (D-CL) catalysts, we see that the citric acid had little influence on the surface concentration of Ni and W as well as on the degree of tungsten sulfidation, i.e., $W^{4+}/(W^{4+} + W^{6+})$. However, the degree of WO_3 sulfidation was significantly lower than that of MoO_3 sulfidation in a nickel–molybdate (4.0 wt.% NiO, 15.5 wt.% MoO_3) catalyst that used the same γ-Al_2O_3 support as used in this work, i.e., $Mo^{4+}/(Mo^{4+} + Mo^{6+}) > 85\%$. For the NiW(cit) (D) catalyst, the surface concentration of W was lowest after sulfidation due to the residual carbonaceous material on the sulfide phases; however, the degree of tungsten sulfidation was comparable to that for the sulfided NiW(cit) (D-L) catalyst. For the sulfided NiW(cit) (D-PY) catalyst, the surface concentrations of Ni and W recovered to the levels for the sulfided NiW(cit) (D-CL) and NiW(am) (D-CL) catalysts. This indicates that pyrolysis produced a similar surface composition to that of the calcined catalysts, in spite of the inhibitory effect of the remaining carbonaceous material on the WS_2-like crystallite formation in the bulk phases. Our results showed no clear indication of the existence of Ni–C and W–C interactions in the sulfided NiW(cit) (D) and NiW(cit) (D-PY) catalysts.

Our XPS results show that the reduction treatment prior to sulfidation minimized the surface Ni/W ratio and the degree of tungsten sulfidation. No metallic phases were detected in either the W4f or Ni2p spectra of the sulfided NiW(cit) (D-CL-R) catalyst.

Table 1
Surface composition of the sulfided catalysts determined using XPS

Catalysts	Relative intensity in atomic ratio to Al					
	Al(%)	S(%)	Ni(%)	W(%)	Ni/W	WS_2(%) [a]
NiW(cit)(D-CL)	100	21.2	5.6	11.8	0.48	60
NiW(cit)(D)	100	17.3	4.4	8.9	0.50	66
NiW(cit)(D-PY)	100	22.2	5.2	12.5	0.42	65
NiW(cit)(D-CL-R)	100	16.3	3.3	10.9	0.30	52
NiW(am)(D-CL)	100	24.4	5.8	12.5	0.46	64

D: dried (393 K); CL: calcined (773 K); PY: pyrolized (773 K); R: reduced (773 K).
[a] Formation of WS_2-like crystallites, $W^{4+}/(W^{4+} + W^{6+}) \times 100$.

3.4. Temperature-programmed reduction (TPR) of the sulfided catalysts

Fig. 3 shows the H_2S formation trends during TPR of the sulfided NiW(cit), NiW(am), and W(cit) catalysts. For comparison, the trends for the sulfided NiMo(cit) (D-CL) are also shown (same γ-Al_2O_3 support as that for the NiW catalysts, i.e., 4.0 wt.% NiO and 15.5 wt.% MoO_3) [6]. For convenience, we divided the H_2S formation pattern into three temperature regions: 300–550 K (region I), 550–930 K (region II), and above 930 K (region III). There are no differences in the EXAFS spectra (Mo K-edge) between the freshly sulfided NiMo(cit) (D-CL) catalyst and sulfided-reduced (up to the end of region I) catalyst. This indicates that the primary H_2S peak (region I) originated from the hydrogenation of the chemisorbed sulfur on coordinatively unsaturated sites of NiMo sulfides. The sulfided W and NiW catalysts exhibited similar behavior. The pattern for the sulfided W(cit) catalyst (Fig. 3a) suggests that the H_2S formation in regions II and III might have originated from the hydrogenation of sulfidic sulfur on the surface and in the bulk parts of the dispersed WS_2-like sulfides, respectively. The patterns for the NiW catalysts (Fig. 3b and c) show that Ni caused an increase in the H_2S formation in all regions. The increase in region I was particularly significant for the NiW(cit) (D-CL) catalyst. A new peak occurred around 880 K in region II for both the NiW catalysts, but was sharper and at a lower temperature for the NiW(cit) catalyst. Citric acid might have contributed to the formation of more dispersed and more uniform Ni–W–S and Ni_3S_2 phases [12] as compared to catalysts prepared by using an ammoniacal method, thus effectively forming S^{2-} coordinatively unsaturated sites. The lower onset temperature for the H_2S formation in region III for the NiW(cit) (D-CL) catalyst compared to that for the NiW(am) (D-CL) catalyst indicates easier reducibility of WS_2-like crystallites in the NiW(cit) (D-CL) catalyst. This lower temperature reproducibility occurred in spite of the more advanced crystallinity of the WS_2-like structure for the NiW(cit) (D-CL) catalyst (as shown by EXAFS). Effective coordination of Ni phases around the WS_2-like crystallites might have promoted the reduction of WS_2-like phases for this catalyst.

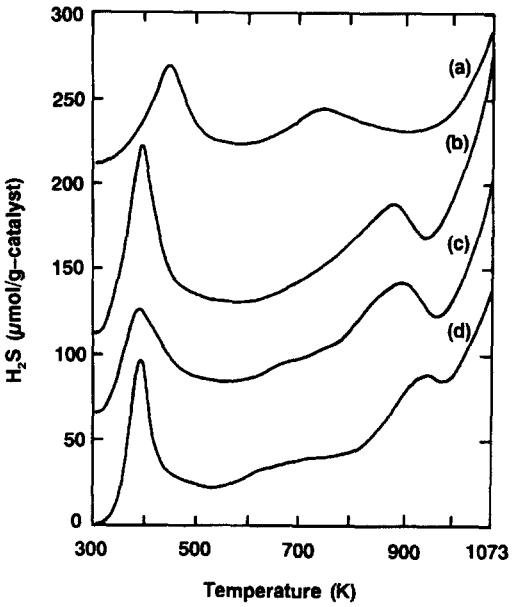

Fig. 3. Profiles of hydrogen disulfide (H_2S) formation during temperature-programmed reduction of the sulfided catalysts: (a) W(cit) (D-CL); (b) NiW(cit) (D-CL); (c) NiW(am) (D-CL); and (d) NiMo(cit) (D-CL).

The temperature dependence of the H_2S formation in region II was more significant for the NiW(cit) catalyst than for the NiMo(cit) catalyst (Fig. 3d). The reason may be linked to the superiority in hydrogenation activity of NiW catalysts to NiMo catalysts under high pressure and temperature reaction conditions. In region III the reducibility of dispersed bulk sulfides was greater for WS_2 than for MoS_2.

3.5. Thermodynamic analyses of the sulfidation and reduction

Thermodynamic analysis was done to better understand the reducibility of Ni, W, and Mo sulfides during TPR, as well as the ease of sulfidation of Ni, W, and Mo oxides during sulfidation.

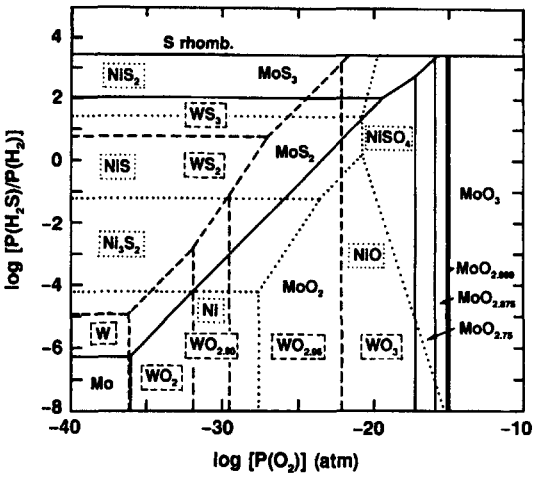

Fig. 4. Chemical potential diagram for the W–O–S, Ni–O–S, and Mo–O–S systems at 673 K: W–O–S (– – –), Ni–O–S (· · ·), and Mo–O–S (—).

The phase relationships among the metal, oxides, and sulfides (e.g., W), can be presented in a three-dimensional chemical potential diagram by using the chemical potentials of μ(S), μ(O) and μ(W) [7]. Similarly, we obtained two-dimensional chemical potential diagrams for the W–O–S system at 673 K as shown in Fig. 4. Here, the y-axis is the ratio of the partial pressure of hydrogen sulfide to that of hydrogen, namely, $P(H_2S)/P(H_2)$, which was calculated from the equilibrium between the gas phases of S_2, H_2S, and H_2 [8]. The x-axis is the partial pressure of oxygen. In the diagram, the vertical line at log $P(O_2) = -22.2$, for example, for the W–O–S system indicates the pressure at which WO_3 will be decomposed into $WO_{2.9}$. The diagrams of Ni–O–S and Mo–O–S systems are also shown in the figure. The right-hand side of the figure [i.e., high $P(O_2)$] represents the oxidizing conditions, and the left-hand side [low $P(O_2)$] represents the reducing conditions.

Reducibility of metal sulfides under the reducing conditions can be evaluated by the equilibrium values for $P(H_2S)/P(H_2)$ between metal sulfides and metals, namely, WS_2–W, Ni_3S_2–Ni, and MoS_2–Mo in Fig. 4. Their reducibility in decreasing order was $Ni_3S_2 > WS_2 > MoS_2$, because the lower the equilibrium value, the stronger the metal–sulfur affinity. This order was the same at elevated temperatures. These results support the reducibility seen in the TPR experiments.

Under the presulfiding conditions (H_2S–H_2; 5:95, v/v), namely, log$[P(H_2S)/P(H_2)] = -1.28$, the components WO_3, NiO, and MoO_3 can be converted into WS_2, Ni_3S_2, and MoS_2, respectively, which are thermodynamically more stable. However, the shifts of the equilibrium lines between oxides and sulfides to more reducing conditions indicate that the sulfidation of oxides became more difficult, namely, the order for sulfidation was $NiO > MoO_3 > WO_3$. This supports the low degree of sulfidation of WO_3 to WS_2 seen in the XPS data.

3.6. Evaluation of the catalytic activities

Fig. 5 shows the effect of calcination temperature on the HYG activities of the NiW catalysts. Analyses of the product gases after the hydrotreatment experiments indicate that values

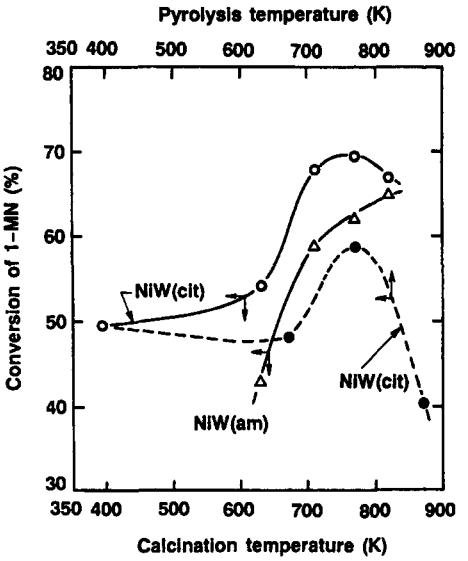

Fig. 5. Effect of calcination and pyrolysis temperatures on the hydrogenation activity of the NiW catalysts where 1-methylnaphthalene (1-MN)–n-hexadecane (30:70, w/w) was used as a reactant.

for the ratio $P(H_2S)/P(H_2)$ were around 2–3 $\times 10^{-3}$, even though no sulfur compounds were added to the tube-bomb batch reactor. This suggests that the formed H_2S was able to maintain the sulfidic states of the active metals, as confirmed thermodynamically. For the NiW(am) (D-CL) catalysts, the HYG activity increased with increasing calcination temperature. This was possibly the cause for the increase in the NiWS I phase [13]. On the contrary, the NiW(cit) (D-CL) catalyst showed higher HYG activity than did the NiW(am) (D-CL) catalyst, and had a maximum around 773 K. It suggests that below 823 K the citrate agent might affect the formation of the NiWS I and II phases; however, solid phase interactions between the active components and the support surface might reach equilibrium around 823 K. The high level of H_2S formation in regions I and II in the TPR experiments were linked with the superiority in the hydrogenation activity of the NiW(cit) (D-CL) catalyst compared with the NiW(am) (D-CL) catalyst. Surprisingly, the NiW(cit) (D) catalyst, which contained about 1.2 wt.% carbon after sulfidation, showed fair HYG activity (about 50% conversion of 1-MN). This level of activity occurred even though we expected little or no effect of the W–O–Al linkages [13]; such linkages might be related to the formation of the NiWS I phase. Pyrolysis of the NiW(cit) (D) catalyst at 773 K resulted in an increase in the HYG activity, though the degree of sulfidation decreased with increasing pyrolyzing temperature (as shown by EXAFS). Further research is necessary to verify the pyrolyzing effect on the structures of the active components.

Fig. 6 shows the initial HYG and HYC activities obtained by the test reactions using DPM. The sulfided NiW(cit) (D-CL) catalyst showed higher HYG activity and higher HYG/HYC selectivity compared with the NiW(am) (D-CL) catalyst. Direct sulfidation of the NiW(cit) (D) catalyst caused a HYG/HYC selectivity similar to that of the NiW(am) (D-CL) catalyst. Reduction pretreatment prior to sulfidation resulted in the lowest HYG activity and lowest HYG/HYC selectivity, but produced the highest amounts of other compounds, which were mainly polymerized products. Refractory in sulfidation of the NiW(D-CL-R) catalyst, as shown in the XPS data, might have contributed to this lowest HYG activity. On the contrary, the sulfided NiW(cit) (D-PY) catalyst, which was pyrolyzed at 773 K, showed higher HYG activity and HYG/HYC selectivity compared with the NiW(cit) (D-CL) catalyst. Pyrolysis of the active components precursors might have contributed not only to the effective S^{2-} site formation on the NiWS II and Ni sulfide [14] phases, particularly at elevated temperatures, but also to neutralization of the catalytic acidity. Therefore, a method using organic complexing agents in the impregnating solutions will have a wide application.

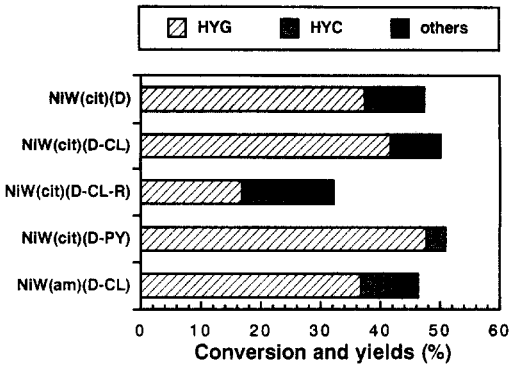

Fig. 6. Hydrogenation and hydrocracking activities of the NiW(cit) and NiW(am) catalysts where diphenylmethane (100 wt.%) was used as a reactant; HYG is the yield of dicyclohexylmethane and benzylcyclohexane, HYC is the yield of benzene and toluene, and others are the yield of polymerized products.

4. Conclusions

From the results of this study, we concluded the following regarding NiW catalysts prepared using our new impregnation method:

(1) Citric acid can be used successfully as a complexing agent in preparing aqueous NiW impregnation solutions, and might be effective in forming polytungstate anions that are smaller than the dodecatungstate anions formed when ammoniacal solutions are used.

(2) Citric acid promotes the effective coordination of nickel around the WS_2-like crystallites. Such coordination might be linked with the ease of S^{2-} vacancy formation during TPR, and thus result in a highly active and hydrogenation selective performance.

(3) Pyrolysis pretreatment of dried NiW(cit) catalysts could increase the hydrogenation selectivity significantly; in particular, hydrotreating reactions at elevated temperatures.

(4) Chemical potential diagrams are useful in predicting trends in the structural changes of active components during sulfidation and reduction.

Acknowledgements

The EXAFS work was performed under the approval of the Photon Factory Program Advisory Committee.

References

[1] C. Gachet, M. Breysse, M. Catteno, T. Decamp, R. Frety, M. Lacroix, L. fe Mourgues, J.L. Portefaix, M. Vrinat, J.C. Duchet, S. Housni, M. Lakhdar, M.J. Tilliette, J. Bachelier, D. Cornet, P. Engelhard, C. Gueguen and H. Toulhoat, Catal. Today, 4 (1988) 7.

[2] A. Nishijima, T. Kameoka, H. Yanase, T. Sato, Y. Yoshimura, H. Shimada and N. Matsubayashi, Proc. Int. Conf. Coal Sci., (1991) 759.

[3] M. Breysse, M. Cattenot, T. Decamp, R. Frety, C. Gachet, M. Lacroix, C. Leclercq, L. de Mourgues, J.L. Portefaix, M. Vrinat, M. Houari, L. Grimblot, S. Kasztelan, J.P. Bonnelle, S. Housni, J. Bachelier and J.C. Duchet, Catal. Today, 4 (1988) 39.

[4] B.H. Cooper, A. Stanislaus, P.N. Hannerup, Am. Chem. Soc. Div. Pet. Chem. Prep., 37 (1992) 41.

[5] J.A.R. Van Veen, E. Gerkema, A.M. van der Kraan and A. Knoester, J. Chem. Soc. Chem. Commun., (1987) 1684.

[6] Y. Yoshimura, N. Matsubayashi, T. Sato, H. Shimada and A. Nishijima, Appl. Catal., 79 (1991) 145.

[7] H. Yokokawa, T. Kawada and M. Dokiya, J. Am. Ceram. Soc., 72 (1989) 2104.

[8] Thermodynamic Database MALT2, Society of Calorimetry and Thermodynamics of Japan, Kagakugijutsusha, Tokyo, 1992.

[9] M.W. Chase, Jr., C.A. Davies, J.R. Downey, Jr., D.J. Frurip, R.A. McDonald and A.N. Syverud, J. Phys. Chem. Ref. Data, 14 (Supplement) (1985).

[10] M.T. Pope and G.M. Varga, Jr., J. Chem. Soc. Chem. Commun., (1966) 653.

[11] H. Shimada, N. Matsubayashi, T. Sato, Y. Yoshimura, M. Imamura, T. Kameoka, H. Yanase and A. Nishijima, Jpn. J. Appl. Phys., 32 (Supplement 32-2) (1992) 463.

[12] P.J. Mangus, A. Bos and J.A. Moulijn, J. Catal., 146 (1994) 437.

[13] R. Candia, O. Sørensen, J. Villadsen, N.-Y. Topsøe, B.S. Clausen and H. Topsøe, Bull. Soc. Chim. Belg., 93 (1984) 763.

[14] A. Miyazawa, J. Tsutui, S. Yoshitomi, T. Sato, Y. Yoshimura, H. Shimada, N. Matsubayashi and A. Nishijima, Sekiyu Gakkaishi, 36 (1993) 291.